Published in final edited form as:

J Mol Cell Cardiol. 2015 October ; 87: 204–213. doi:10.1016/j.yjmcc.2015.08.018.

Cardiac-specific deletion of protein phosphatase 1β promotes increased myofilament protein phosphorylation and contractile alterations

Ruijie Liu[a], **Robert N. Correll**[a], **Jennifer Davis**[a], **Ronald J. Vagnozzi**[a], **Allen J. York**[a], **Michelle A. Sargent**[a], **Angus C. Nairn**[b], and **Jeffery D. Molkentin**[a]

[a]Department of Pediatrics, University of Cincinnati, Cincinnati Children's Hospital Medical Center, Howard Hughes Medical Institute, Cincinnati, OH 45229, USA

[b]Department of Psychiatry, Yale University School of Medicine, New Haven, CT 06520 USA

Abstract

There are 3 protein phosphatase 1 (PP1) catalytic isoforms (α, β and γ) encoded within the mammalian genome. These 3 gene products share ~90% amino acid homology within their catalytic domains but each has unique N- and C-termini that likely underlie distinctive subcellular localization or functionality. In this study, we assessed the effect associated with loss of each PP1 isoform in the heart using a conditional Cre-loxP targeting approach in mice. *Ppp1ca-loxP, Ppp1cb-loxP* and *Ppp1cc-oxP* alleles were crossed with either an *Nkx2.5-Cre* knock-in containing allele for early embryonic deletion or a tamoxifen inducible α-myosin heavy chain (αMHC)-MerCreMer transgene for adult and cardiac-specific deletion. We determined that while deletion of *Ppp1ca* (PP1α) or *Ppp1cc* (PP1γ) had little effect on the whole heart, deletion of *Ppp1cb* (PP1β) resulted in concentric remodeling of the heart, interstitial fibrosis and contractile dysregulation, using either the embryonic or adult-specific Cre-expressing alleles. However, myocytes isolated from *Ppp1cb* deleted hearts surprisingly showed enhanced contractility. Mechanistically we found that deletion of any of the 3 PP1 gene-encoding isoforms had no effect on phosphorylation of phospholamban, nor were Ca^{2+} handling dynamics altered in adult myocytes from *Ppp1cb* deleted hearts. However, loss of *Ppp1cb* from the heart, but not *Ppp1ca* or *Ppp1cc*, resulted in elevated phosphorylation of myofilament proteins such as myosin light chain 2 and cardiac myosin binding protein C, consistent with an enriched localization profile of this isoform to the sarcomeres. These results suggest a unique functional role for the PP1β isoform in affecting cardiac contractile function.

Corresponding author: Jeffery D. Molkentin, Cincinnati Children's Hospital Medical Center, Howard Hughes Medical Institute, Molecular Cardiovascular Biology, 240 Albert Sabin Way, MLC 7020, Cincinnati, Ohio 45229, USA. jeff.molkentin@cchmc.org.

Disclosures

No financial or other conflicts of interest exist with any of the authors.

Keywords

protein phosphatase 1; myofilament protein; contractility; heart failure

1. Introduction

Protein phosphatase 1 (PP1) is a serine/threonine phosphatase that plays a fundamental role in many cellular processes [1]. The three isoforms of the catalytic subunits (PP1α, PP1β, and PP1γ) are encoded by distinct genes that are highly homologous to one another, although their divergent N- and C-termini are believed to underlie some diversification in target selectivity [2–4]. However, isoform-specific regulation and functions of specific PP1 isoforms are complex and remain poorly understood. For example, PP1α and PP1γ have been reported to selectively interact with neurabin to target the actin cytoskeleton [5, 6], although this interaction specificity is not likely due to the more divergent N- or C-termini of PP1 [7]. PP1β also forms a selective complex with the targeting subunit 2 of myosin phosphatase (MYPT2) [8]. In the heart, increased PP1 activity is implicated in heart failure progression, and PP1β was reported to be preferentially associated with the sarcoplasmic reticulum (SR) where it influences Ca^{2+} cycling [9, 10].

Dynamic phosphorylation and dephosphorylation of key regulatory proteins is a major determinant of cardiac Ca^{2+} cycling and myofilament protein force production and cross-bridge cycling. For example, sympathetic stimulation generates cAMP in the heart that activates protein kinase A (PKA) resulting in the phosphorylation of nodal Ca^{2+} handling proteins, such as ryanodine receptor 2 (RyR2) and phospholamban (PLN), which then augment contractility and lusitropy to facilitate greater cardiac output [11, 12]. Several myofilament proteins are also regulated at the level of phosphorylation to affect contractile or lusitropic activity [8, 13], such as myosin light chain 2V (MLC2V) at serine 14/15 by the myosin light chain kinase (MLCK) [14, 15]. Indeed, transgenic mice overexpressing a phosphorylation-deficient MLC2V mutant protein in the heart showed aberrant cardiac function [16, 17]. Cardiac myosin binding protein C (cMyBPC), a 140-kDa thick filament protein that regulates the binding of the myosin head to actin [18], can be phosphorylated at serines 273/282/302 by PKA, protein kinase C and Ca^{2+}/calmodulin-dependent kinase [19]. Transgenic mice overexpressing phosphorylation deficient or phosphomimetic cMyBPC mutant proteins in the heart demonstrate that phosphorylation of this protein is a critical regulatory mechanism for altering cardiac function [20], and very similar observations have also been made for phosphorylation of the troponin proteins in the heart [21, 22].

Given the pro-contractile effects associated with kinase-mediated phosphorylation of select myofilament proteins, regulated inhibition of protein phosphatases is hypothesized to maintain or augment this sympathetic “fight-or-flight” profile of catecholamine-mediated protein phosphorylation. Indeed, studies of inhibitor-1 and inhibitor-2, proteins that specifically inactivate PP1, support such a relationship. For example, overexpression of either inhibitor-2 [23] or a constitutively active inhibitor-1 mutant [24] in the hearts of transgenic mice resulted in increased cardiac function. Conversely, overexpression of a catalytic PP1α isoform in the heart led to reduced cardiac function and heart failure [11].

However, other data generated in mice where PP1 activity has been manipulated suggest a more complicated picture, such that inhibition of PP1 by overexpression of inhibitor-2 led to more severe heart failure in mice with pressure overload [25], while inhibitor-1 overexpressing transgenic mice showed cardiac hypertrophy with depressed cardiac function [26]. Thus, despite the clear nodal position of PP1 in regulating cardiac function, it remains unclear how this phosphatase might be modulated to treat heart disease [27], although one attractive possibility is to more selectively target only one of the 3 known PP1 gene-encoding isoforms: *Ppp1ca* (PP1α), *Ppp1cb* (PP1β), or *Ppp1cc* (PP1γ).

In the present study, we employed a novel approach to address this long-standing issue as to how PP1 activity might be manipulated to affect cardiac contractility and propensity towards heart failure. We employed Cre-loxP technology to achieve cardiac-specific deletion of each of the 3 PP1 gene isoforms in the mouse. Our results show that while deletion of PP1α or PP1γ had no effect on the heart at baseline, loss of PP1β promoted ventricular remodeling and heart failure, in association with a dramatic change in myofilament protein phosphorylation, but without a change in Ca^{2+} handling dynamics or PLN phosphorylation.

2. Materials and Methods

2.1. Mice and tamoxifen administration

All mice were bred and utilized according to procedures approved by the Animal Care and Use Committee at the Cincinnati Children's Hospital Medical Center. *Ppp1cα-loxP* (*fl*), *Ppp1cb-fl*, and *Ppp1cc-fl* mice, in which exon 3 was flanked by Cre recombinase-dependent loxP recognition sequences, were generated in collaboration with Lexicon Genetics as described previously [28]. These mice were then crossed with the Cre recombinase knock-in line *Nkx2.5-Cre* [29] or the tamoxifen-inducible α-myosin heavy chain (αMHC)-MerCreMer transgene [30] to achieve efficient deletion of each PP1 isoform in the heart. Tamoxifen (Sigma, T-5648) was dissolved in peanut oil (5 mg/ml) and administered to *Ppp1c*$^{\alpha MHC\text{-}MerCreMer}$ mice via intraperitoneal (IP) injections for five consecutive days (0.5 mg/day), after which mice were analyzed 2, 6, and 8 weeks later.

2.2. Isolation of adult mouse cardiomyocytes

Adult ventricular myocytes were isolated as described previously [31]. In brief, hearts from 2 month-old mice were removed after treatment with heparin (0.35 units) under anesthesia (Nembutal, 100 mg/kg), and cannulated for retrograde perfusion with a solution containing liberase blendzyme (Roche, 05401151001) followed by a gentle mechanical disassociation using sterile plastic pipettes to generate individual myocytes. After transferring to a new tube, myocytes were allowed to settle by gravity followed by $CaCl_2$ re-introduction. The cell pellet was resuspended in MEM (Modified Eagles Medium) plus 5% fetal bovine serum, and cells were counted and plated on laminin-coated dishes.

2.3. Ventricular myocyte protein subfractionation

Subcellular protein fractions were prepared as described previously [32]. In brief, cells were washed and collected in lysis buffer containing 50 mM Tris-HCl pH 7.4, 5 mM EGTA, 2 mM EDTA, 5 mM DTT, 0.05% digitonin, and a protease/phosphatase inhibitor cocktail

(Thermo Fisher Scientific, 78440). Cell lysates were centrifuged at 14,000 x g for 15 min, and the supernatant was collected as a cytosolic fraction. The pellet was resuspended in lysis buffer containing 1% Triton x-100 for 10 min and centrifuged for 15 min at 14,000 x g to collect the supernatant as the membrane fraction. The subsequent triton-insoluble pellet contained the myofilament fraction. This insoluble pellet was resuspended with PBS buffer containing 0.5 M NaCl for 20 min on ice and centrifuged to collect supernatant as the final myofilament protein fraction. Protein samples from each fraction were quantified with a Bradford assay (Bio-Rad) and subjected to 10% SDS-PAGE for Western blot detection of PP1α (Santa Cruz Biotechnology, sc-6104), PP1β (Millipore, 07-1217), PP1γ (Santa Cruz Biotechnology, sc-6108), GAPDH (Fitzgerald, 10-1500), Troponin I (Cell Signaling Technology, 4002), pSer 23/24-Troponin I (Cell Signaling Technology, 4004), Caveolin-3 (BD Biosciences, 610421), I-1 (Abcam, ab40877), and I-2 (R&D Systems, AF4719).

2.4. Myofilament protein isolation, Pro-Q Diamond staining and Phos-Tag Westerns

Mouse hearts were minced into small pieces with scissors and homogenized in F60 solution (60 mM KCl, 30 mM imidazole, 2 mM $MgCl_2$, and a protease/phosphatase inhibitor cocktail (Thermo Fisher Scientific, 78440)). Tissues were collected by centrifugation for 3 minutes at 8,000 x g, resuspended in F60 solution two more times, followed by 2 washes with F60 solution containing 1% Triton x-100. The pellet was washed 3 times with F60 and eluted with buffer (20 mM HEPES, 1% Triton, 0.5 M NaCl, 1 mM EDTA, and a protease/phosphatase inhibitor cocktail (Thermo Fisher Scientific, 78440)). Protein samples were quantified and equal amounts of protein was subjected to 12% SDS-PAGE. For Pro-Q Diamond staining, the acrylamide gel containing the separated proteins were fixed, washed and stained with Pro-Q Diamond solution (Invitrogen, P-33300). Images were visualized through UV transillumination (Bio-Rad). For Phos-Tag gels, Phos-Tag (Wako Chemicals, 304-93526) and $MnCl_2$ solution were added to the 12% acrylamide gel to reach a final concentration of 50 μM, and 0.1 mM respectively. The gel was washed with transfer buffer containing 1 mM EDTA, transferred, and blotted with MLC2V antibody (Proteintech, 10906-1-AP).

2.5. Ca^{2+} and cell shortening measurements

Ca^{2+} measurement assays in adult cardiac myocytes have been described previously [33]. In brief, cells were loaded with 2 μM Fura-2 acetoxymethyl ester (Invitrogen, C-2938) for 15 min, and then placed in Tyrode's solution containing: 130 mM NaCl, 4 mM KCl, 2 mM $CaCl_2$, 1 mM $MgCl_2$, 10 mM glucose and 10 mM HEPES (pH 7.4). The Fura-2 fluorescence ratio was determined with a Delta scan dual-beam spectrofluorophotometer (Photon Technology International) operated at an emission wavelength of 510 nM and excitation wavelengths of 340 and 380 nM. The myocyte stimulation frequency for Ca^{2+} transient measurements was 0.5 Hz. For caffeine-induced Ca^{2+} release, myocytes were perfused with a Tyrode's solution and stimulated at 0.5 Hz until stabilization of the transients, after which caffeine was acutely added. Ca^{2+} traces from healthy myocytes sensitive to caffeine treatment were processed using a Savitzky-Golay filter and baseline Ca^{2+} levels, transient amplitude, caffeine-induced Ca^{2+} release, and Ca^{2+} decay kinetics were analyzed using Felix 1.1 and Ion Wizard (IonOptix) software. For cell shortening measurements in isolated adult myocytes, cells were bathed in media 199 (M199) at room temperature using an

Ionoptix system as described previously [34, 35] and myocytes were electrically paced at 0.5 Hz with 60V and the solution was refreshed between each measurement.

2.6. Cardiac catheterization and echocardiography

Mice were anesthetized by IP injection of pentobarbital (6 mg/100 g body weight). A high fidelity, solid state 1.2F pressure-volume catheter (Transonic Systems Inc, FTH-1212B-3518) was inserted into the left ventricle via a right carotid exposure and retrograde introduction of the catheter into the left ventricle. The signal was optimized by phase and magnitude channels [36]. Data were collected with a PowerLab 8/36 (ADInstruments) work station and analyzed using LabChart 7 Pro (ADInstruments). Dobutamine (NDC 0338-1073-02) was infused into the right jugular by syringe pump (KD Scientific, KDS210) as described previously [37].

Echocardiography was performed as described previously [38]. In brief, mice were anesthetized by 2% isoflurane inhalation. Two-dimensional guided M-mode tracings of a cross section of the left ventricle (LV) minor axis at the tip of the papillary muscles were obtained using a SONOS 550 instrument (Hewlett-Packard) with a 15-MHz transducer. Fractional shortening (FS) was calculated using left ventricle diameters in the end of systole and diastole (LVIDs and LVIDd, respectively) according to the formula: ([LVIDd-LVIDs]/LVIDd)×100(%).

In a separate set of experiments, mice were lightly anesthetized by 0.8–1% isoflurane inhalation and analyzed by B-mode and M-mode echocardiography using a Vevo2100 instrument with an 18–38 MHz transducer (VisualSonics). Short axis M-mode traces across the mid-papillary region of the LV were collected and LV dimensions averaged over a minimum of five consecutive cardiac cycles per heart were analyzed to determine ejection fraction (EF) according to the formula: EF(%)=100*[(LVED–LVES)/LVED], where LVED=[7.0/(2.4+LVIDd)]*(LVIDd)^3 and LVES= [7.0/ (2.4+LVIDs)]*(LVIDs)^3. Abbreviations, LVED, left ventricular end-diastolic volume; LVES, left ventricular end-systolic volume; LVIDd, left ventricular end-diastolic diameter; LVIDs, left ventricular end-systolic diameter.

2.7. Quantitative PCR

Total RNA was isolated from mouse hearts or adult cardiac myocytes using the RNeasy Fibrous Tissue Kit (Qiagen, 74704), and quantified using a NANODROP 2000 Spectrophotometer (Thermo Scientific). cDNA was synthesized using the SuperScript III First-Strand Synthesis Kit (Invitrogen, 18080-051). Quantitative PCR was performed using SYBR green dye (Bio-Rad, 172-5274) on a CFX96 Real-Time PCR Detection System (Bio-Rad). The primer sequences for real-time PCR were as follows: *Ppp1ca*, forward: 5’-cctccagagagcaactacctcttc-3’, reverse: 5’-acgtcttccacagtttgatgttgt-3’; *Ppp1cb*, forward: 5’-aatatggaggttttccaccagaag-3’, reverse: 5’-attgatgctagcacactcatggtt-3’; *Ppp1cc*, forward: 5’-tcttcctcagtcagcctatccttt-3’, reverse: 5’-ctccggatacttgattttgtaggc-3’; matrix metalloproteinase-2 (MMP2), forward: 5’-gtcgcccctaaaacagacaa-3’, reverse: 5’-ggtctcgatggtgttctggt-3’; collagen 1α1, forward: 5’- gagcggagagtactggatcg-3’, reverse: 5’-

gcttcttttccttggggttc-3'; ribosomal protein 27, forward: 5'-ggacgctactccggacgcaaag-3', reverse: 5'-cttcttgcccatg gcagctgtcac-3'.

2.8. Statistics

All the results are presented as mean ± SEM. Statistical analysis was performed using Microsoft Excel using Student's t-test for 2 group analysis or ANOVA followed by a Bonferroni post hoc test for comparison of differences across multiple groups,. $P<0.05$ was considered statistically significant.

3. Results

3.1 Generation of cardiac-specific PP1 isoform deleted mice

We first analyzed endogenous expression of each PP1 isoform in isolated mouse ventricular myocytes to begin to investigate their potential unique functional roles. Through quantitative PCR we determined that expression of PP1β (*Ppp1cb* gene) was significantly higher than PP1α (*Ppp1ca* gene) or PP1γ (*Ppp1cc* gene) (Fig. 1A). Next, to achieve cardiac-specific deletion of each PP1 isoform in the heart we used mice that were genetically targeted with loxP (fl) sites for all three genes; *Ppp1ca-fl/fl*, *Ppp1cb-fl/fl*, and *Ppp1cc-fl/fl* and subsequently crossed each with *Nkx2.5-Cre* knock-in mice, which drives Cre expression early in the developing heart proceeding through adulthood [29, 39]. Mice with *Nkx2.5-Cre*-mediated deletion of each of the *Ppp1c* isoforms were viable and showed normal lifespans, suggesting that the individual PP1 isoforms are not separately required for heart development or adult viability. Quantitative PCR and Western blotting showed efficient reductions of each PP1 isoform in the heart due to the *Nkx2.5-Cre* knock-in allele (Figs. 1B–D). Interestingly, reduction of PP1α led to a slight increase of PP1β protein expression, and reduction of PP1β caused up-regulation of PP1α and PP1γ protein levels, suggesting that there is compensation between these 3 isoforms in the heart (Figs. 1C, D). Inhibitor 1 (I-1), the endogenous protein inhibitor of PP1, was significantly reduced upon *Ppp1cb* deletion, while inhibitor 2 (I-2) levels were not affected in any of the PP1 isoform deficient mice (Figs. 1C, D).

To examine the potential functional effects associated with deletion of each PP1 isoform from the heart we first performed echocardiography in young adult mice. M-mode measurements in 2 month-old mice showed increased cardiac FS, reduced ventricular chamber dimension, and increased septal thicknesses in *Ppp1cb-fl/fl*$^{Nkx2.5\text{-}Cre}$ mice, but not *Ppp1ca-fl/fl*$^{Nkx2.5\text{-}Cre}$ or *Ppp1cc-fl/fl*$^{Nkx2.5\text{-}Cre}$ mice (Figs. 2A–D). In addition, heart rate in *Ppp1cb-fl/fl*$^{Nkx2.5\text{-}Cre}$ mice was significantly lower compared to the *Nkx2.5-Cre* knock-in allele containing mice (402.76±20 vs 472.85±11 respectively, $P<0.05$). However, the LV posterior wall thicknesses were not different between the Cre controls and any of the *Nkx2.5-Cre*-targeted PP1 deleted mice (Fig. 2C).

To further validate the functional measurements obtained by echocardiography, we compared the cell size, contraction amplitude and velocity in isolated adult cardiomyocytes from *Ppp1cb-fl/fl* or *Ppp1cb-fl/fl*$^{Nkx2.5\text{-}Cre}$ mice. Myocytes from the hearts of *Ppp1cb-fl/fl*$^{Nkx2.5\text{-}Cre}$ mice demonstrated increased width, consistent with the increased septal sickness

in *Ppp1cb-fl/fl*$^{Nkx2.5\text{-}Cre}$ mice (Fig. 2E). In addition, cardiomyocytes from *Ppp1cb-fl/fl*$^{Nkx2.5\text{-}Cre}$ mice had increased shortening amplitude (Fig. 2F), consistent with increased FS by echocardiography measured in the mice. Shortening velocity was not altered by PP1β isoform loss, but the relaxation velocity was enhanced (Figs. 2G, H). Together, PP1β loss in the heart leads to enhanced cardiac performance by echocardiography and in isolated myocytes, indicating a functional effect for protein phosphorylation as regulated by this phosphatase isoform on contractile performance.

3.2 Deletion of Ppp1cb by Nkx2.5-Cre uniquely leads to heart failure

Given the enhanced cardiac contractile performance profile observed with PP1β deletion as measured by echocardiography and in isolated adult myocytes, we next analyzed mice with cardiac PP1 isoform deletions for cardiac histological features of remodeling or any overt structural alterations. As shown above (Fig. 2D), deletion of *Ppp1cb* with the *Nkx2.5-Cre* allele promoted concentric ventricular remodeling but this did not lead to a net increase in total heart weight normalized to body weight at 2 months of age, nor did deletion of *Ppp1ca* or *Ppp1cc* (Fig. 3A). However, only *Ppp1cb-fl/fl*$^{Nkx2.5\text{-}Cre}$ mice had increased atria-to-body weight ratios, as well as increased lung-to-body weight ratios compared to either control mice or PP1α or PP1γ cardiac-deficient mice at 2 months of age (Figs. 3B, C). These later results were initially perplexing because they suggested a heart failure or decompensated profile. Indeed, significantly augmented interstitial fibrosis in conjunction with increased expression of collagen 1α1 and matrix metalloproteinase-2 (MMP-2) were observed in hearts from *Ppp1cb-fl/fl*$^{Nkx2.5\text{-}Cre}$ mice, while loss of either PP1α or PP1γ had no effect at 2 months of age (Figs. 3D–G).

Since deletion of *Ppp1cb* in the heart appeared to increase contractility with some measures, and yet resulted in histological and biochemical features of cardiac dysfunction, we further assessed cardiac contractility with invasive hemodynamics using a pressure-volume catheter in 2 month-old mice. Consistent with histological observations, *Ppp1cb-fl/fl*$^{Nkx2.5\text{-}Cre}$ hearts had decreased contractility by invasive hemodynamic assessment, while *Ppp1ca-fl/fl*$^{Nkx2.5\text{-}Cre}$ and *Ppp1cc-fl/fl*$^{Nkx2.5\text{-}Cre}$ had no alterations (Fig. 4A). *Ppp1cb-fl/fl*$^{Nkx2.5\text{-}Cre}$ mice also uniquely showed reduced cardiac diastolic performance and compromised relaxation (Figs. 4B, C). In addition, *Ppp1cb-fl/fl*$^{Nkx2.5\text{-}Cre}$ mice had slightly reduced heart rates, and likely as compensation to this reduction, stroke volume was increased so that cardiac output (CO) was not changed (Figs. 4D–F). Taken together, these results suggest that deletion of PP1β produces a net deficit in whole organ cardiac contractility as assessed by invasive hemodynamics, most likely due to the observed remodeling phenotype of increased septal thickness, fibrosis and reduced LV chamber dimension, which by echocardiography actually produced a profile of greater FS. This increase in FS by echocardiography likely reflects changes in heart geometry and a reduced heart rate that secondarily generated greater ventricular filling with more forceful ventricular shortening. However, individual myocytes from hearts deficient in *Ppp1cb* showed some aspects of enhanced contractile activity at 2 months of age. Hence, loss of PP1β from the heart positively and negatively impacted measures of cardiac functional performance depending on the assessment used and its limitations or strengths (see discussion).

Using shRNAs to knock-down each PP1 isoform in isolated adult cardiac myocytes, a recent study suggested that PP1β is the major isoform regulating SR Ca^{2+} cycling by directly affecting PLN phosphorylation [10]. This previous study showed that reduced expression of PP1β enhanced contractile performance of individual myocytes, which we also observed as presented above, although our study uniquely assessed the more global effect in mice when this gene was deleted from the entire heart and the secondary effects associated with remodeling.

3.3 PP1β is localized to the sarcomere to regulate myofilament proteins

To further investigate a mechanism whereby loss of PP1β from the heart might alter cardiac remodeling and impact cardiac contractile activity, we analyzed PLN phosphorylation in 2 month-old mice at baseline as well as upon 10 min of isoproterenol challenge. PLN phosphorylation was not affected by deletion of any of the PP1 isoforms in comparison to Cre controls (Figs. 5A, B, Suppl. Figs. 1A–D). To further examine PLN phosphorylation *in vivo*, we also used cardiac myocytes isolated from 6 week-old mice. Despite the previous report in the literature [10], PLN phosphorylation at serine 16 or threonine 17 was not increased or otherwise affected in the hearts of mice lacking PP1β protein, similar to a lack of effect in the absence of PP1α or PP1γ protein (Suppl. Figs. 2A, B).

To examine changes in other phosphorylated substrates as potential molecular mechanisms for the cardiac alterations observed in *Ppp1cb-fl/fl*$^{Nkx2.5\text{-}Cre}$ mice, we investigated the localization of PP1β by subcellular fractionation of protein extracts from adult cardiac myocytes. All 3 PP1 isoforms were localized to the cytoplasm and membrane, although PP1β was the only isoform more preferentially localized to the myofilament protein-containing fraction (Fig. 5C), possibly due to binding to its targeting subunit MYPT2 [8]. Interestingly, I-1 and I-2 were also localized to the myofilament fraction (Fig. 5C). To further confirm the myofilament localization of each PP1 isoform, we generated myofilament fractions from hearts of mice lacking PP1 protein isoforms (Fig. 5D). Protein levels of each PP1 isoform were reduced in their respective deleted genotype, and loss of PP1β was again compensated by an increase of the PP1α protein, similar to the results obtained from total heart cytosolic protein lysates presented earlier (Fig. 1C). Interestingly, I-1 was significantly reduced in the myofilament fraction from PP1β deficient mice, suggesting that the expression of these two proteins were co-regulated at this location.

We also extracted myofilament proteins from hearts of 2 month-old mice of each of the isoform-specific deleted groups and the control group, and detected their global phosphorylation status by Pro-Q Diamond reactivity, which selectively marks phosphorylated proteins. Here we observed elevated phosphorylation of MLC2V at baseline in PP1β protein deficient hearts, but not in PP1α or PP1γ protein deficient hearts (Fig. 5E, upper gel). Unfortunately, a lack of commercially available antibodies for phosphorylation sites in MLC2V prevented a more exact analysis of all the potential sites. However, to confirm the result obtained from Pro-Q Diamond gels, we utilized the Phos-Tag gel system to detect migration shifts due to protein phosphorylation (see Methods). A major shift in MLC2V was observed in heart samples from *Ppp1cb-fl/fl*$^{Nkx2.5\text{-}Cre}$ mice, but not *Ppp1ca-fl/fl*$^{Nkx2.5\text{-}Cre}$ or *Ppp1cc-fl/fl*$^{Nkx2.5\text{-}Cre}$ mice, again suggesting enhanced MLC2V

phosphorylation (Fig. 5E, lower panel; Suppl. Fig. 3A). Previous studies have suggested ser14/15 in rodents and ser15 in human as the phosphorylation sites in MLC2 [15, 40]. In our study with the Phos-Tag gel system we observed two distinct protein bands for MLC2, which likely correlate with unphosphorylated and doubly phosphorylated MLC2 at ser14/15 [40]. Phosphorylation of troponin I, at ser 23/24 was not altered in any of the PP1 isoform deficient mouse hearts (Fig. 5E, lower panel), consistent with a previous study using PP1 siRNAs to examine the role of PP1 isoforms in isolated adult rat cardiomyocytes [10]. Upon stimulation of the mice with isoproterenol for 10 minutes, we did not observe a further increase of MLC2 phosphorylation (Suppl. Fig. 3B). However, we observed increased phosphorylation of cMyBPC in the hearts of *Ppp1cb-fl/fl*$^{Nkx2.5\text{-}Cre}$ mice (Suppl. Fig. 3B), which was further revealed by phosphorylation specific antibodies against serines 273/282/302 of cMyBPC (Fig. 5F). Together, these data indicate that PP1β regulates myofilament protein phosphorylation that likely secondarily influences cardiac contractility or relaxation.

3.4 Adult deletion of Ppp1cb with αMHC-MerCreMer also alters heart parameters

The adult cardiac phenotype observed in *Ppp1cb-fl/fl*$^{Nkx2.5\text{-}Cre}$ mice could have been influenced by one of more developmental effects during embryogenesis given the known early expression profile of the *Nkx2.5-Cre* knock-in allele. To address this issue we also crossed each of the *Ppp1c-loxP* mice with a tamoxifen-inducible *aMHC-MerCreMer* transgenic line to achieve adult-specific deletion in the heart as previously characterized [41, 42]. To induce gene deletion, mice were given five consecutive days of IP injection of tamoxifen (0.5 mg/day) (Fig. 6A), and PP1 isoform deletion and cardiac function were analyzed either 2 or 6 weeks later. At 14 weeks of age, Western blotting for protein expression showed that each PP1 isoform was significantly reduced from the heart 6 weeks after the tamoxifen injection regimen (Fig. 6B). We also observed compensatory upregulation of PP1β protein in *Ppp1ca-flfl*$^{aMHC\text{-}MerCreMer}$ hearts, as well as an increase in PP1α or PP1γ protein in *Ppp1cb-fl/fl*$^{aMHC\text{-}MerCreMer}$ hearts (Fig. 6B, and Suppl. Figs. 4B). Also consistent with the data presented earlier, echocardiographic assessment of the heart demonstrated increased FS in *Ppp1cb-fl/fl*$^{aMHC\text{-}MerCreMer}$ mice (Fig. 6C), as well as mild fibrosis compared to control and PP1α or PP1γ protein-deleted mice (Fig. 6D). Similarly, mice 2 weeks after tamoxifen treatment also showed a significant reduction of each PP1 isoform and the same profile of compensated increases of other PP1 isoforms (Fig. 6E, and Suppl. Fig. 4A). *Ppp1cb-fl/fl*$^{aMHC\text{-}MerCreMer}$ also demonstrated increased FS as soon as 2 weeks after tamoxifen treatment (Fig. 6F). However, compared with the overt cardiac phenotypes observed upon deletion of PP1β by the Nkx2.5 driven Cre, adult deletion of PP1β resulted in milder changes (Suppl. Table 1). We also analyzed cardiac performance 8 weeks after tamoxifen injection, which showed significant increases in atria-to-body weight ratios in *Ppp1cb-fl/fl*$^{MHC\text{-}MerCreMer}$ mice compared to controls, without changes in heart weight-to-body weight ratios (Suppl. Figs. 5A,B), consistent with the phenotype in *Ppp1cbfl/fl*$^{Nkx2.5\text{-}Cre}$ mice (Fig. 3B). Also consistent, echocardiography assessment of FS or ejection fraction, as independently analyzed with the highly sensitive Vevo2100 small animal echocardiography system, were elevated in *Ppp1cb-fl/fl*$^{aMHC\text{-}MerCreMer}$ mice (Suppl. Figs. 5C, D).

3.5 Adult specific Ppp1cb deletion also preferentially affects myofilament protein phosphorylation

We again assessed PLN phosphorylation upon deleting each PP1 isoform, but this time from the adult heart (14 weeks of age). Compared to control αMHC-MerCreMer transgene only mice, mice with adult-specific deletion of each of the PP1 isoforms did not show altered PLN phosphorylation in the heart, as well as in isolated adult cardiomyocytes (Fig. 7A, Suppls. Figs.1 E–H, and Suppls. Figs. 2C, D). Given that an increase in PLN phosphorylation was previously suggested to underlie a change in cardiac Ca^{2+} handling and contractility with PP1β-shRNA-mediated knockdown [10], we also assessed Ca^{2+} dynamics from myocytes isolated from hearts of *Ppp1cb-fl/fl*$^{aMHC\text{-}MerCreMer}$ mice. However, we observed no change in the Ca^{2+} transient or SR Ca^{2+} load between *Ppp1cb-fl/fl*$^{aMHC\text{-}MerCreMer}$ and αMHC-MerCreMer control mice (Figs. 7B–D). These data indicate that loss of the PP1β protein from the heart does not alter Ca^{2+} handling. However, using ProQ Diamond or Phos-Taq gel analysis we again observed increased MLC2 phosphorylation in the absence of PP1β protein in the heart, but we observed no effect with loss of PP1α or PP1γ (Fig. 7E). We also observed a similar increase in cMyBPC protein phosphorylation in the absence of PP1β protein (but not PP1α or PP1γ) from the adult heart at serines 282 and 302 (data not shown).

To again carefully assess cardiac contractile function we performed invasive hemodynamic measurements in a close-chested preparation in the mouse (Fig. 7F, and Suppl. Table 2). Heart rates between control and *Ppp1cb-fl/fl*$^{aMHC\text{-}MerCreMer}$ mice were not significantly different (464 ±13.2 vs 475±17.0, respectively). However, the data showed a rightward shift of the pressure-volume curve upon *Ppp1cb* deletion, suggestive of diastolic alterations in these mice, but not failure. ESPVR, a measurement of systolic properties [43], was similar between *Ppp1cb-fl/fl*$^{aMHC\text{-}MerCreMer}$ and control mice, but the EDPVR showed augmented relaxation in *Ppp1cb-fl/fl*$^{aMHC\text{-}MerCreMer}$ mice without a change in stroke volume. This increase in EDPVR is similar to the enhanced relaxation rate observed in isolated cardiomyocytes presented earlier, in the absence of PP1β (Fig. 2G), which is also consistent with how increased phosphorylation of myofilament proteins might affect cardiac contractile performance. However, upon dobutamine challenge, *Ppp1cb-fl/fl*$^{aMHC\text{-}MerCreMer}$ mice demonstrated blunted responsiveness compared to αMHC-MerCreMer mice (Suppl. Fig. 6), suggestive of β-adrenergic deficiency that is also consistent with fibrosis in these hearts (Fig. 6D) and the antecedents of cardiac dysfunction that were more fulminant when the more potent *Nkx2.5-Cre* was used to delete PP1β (also given embryonic loss of PP1β that appears to have a more long-term negative effect). The heart rate was similar between control and *Ppp1cb-fl/fl*$^{aMHC\text{-}MerCreMer}$ mice, suggesting that the blunted β-adrenergic responsiveness was not associated with heart rate alterations (Suppl. Fig. 6C). Finally, isolated adult ventricular myocytes again showed an increase in cellular width, consistent with a phenotype of concentric remodeling of the heart in the absence of PP1β protein (Fig. 7G).

4. Discussion

Protein phosphatase 1 is one of the major serine/threonine phosphatases in the heart that has been suggested as a potential therapeutic target for heart disease treatment through effects on

numerous downstream targets [44, 45]. In the current study we successfully achieved deletion of each PP1 isoform by crossing *Ppp1c-fl/fl* mice with either the *Nkx2.5-Cre* knock-in allele or the inducible *aMHC-MerCreMer* transgene containing mice. Through functional measurements and biochemical analysis we demonstrated that: 1) PP1β is the predominant isoform expressed in ventricular myocytes and the major isoform targeted to the myofilament where it regulates phosphorylation of MLC2V and cMyBPC. 2) Individual deletion of PP1 isoforms from the heart does not affect PLN phosphorylation, or the Ca^{2+} transient in myocytes. 3) PP1β deletion leads to enhanced contractile responses in isolated adult myocytes, but the whole heart demonstrates cardiac concentric remodeling, fibrosis, and reduced contractility at baseline and upon dobutamine challenge.

Previously, PP1β was suggested to be the major isoform regulating SR Ca^{2+} handling and cardiac contractile performance. Knockdown of PP1β by shRNA in rat cardiomyocytes enhanced PLN phosphorylation and Ca^{2+} transients at baseline and with isoproterenol stimulation, and increased cell shortening [10]. Furthermore, the same group demonstrated that suppression of PP1β by adeno-associated vial 9 encoded shRNA gene delivery to the heart improved cardiac function in muscle LIM protein (MLP) deficient mice (*Csrp3* gene), which have a cardiomyopathy phenotype [46]. Our current observations are only partially at odds with these 2 previous reports, as deletion of *Ppp1ca*, *Ppp1cb* or *Ppp1cc* had no effect on PLN phosphorylation or the Ca^{2+} transient from adult cardiomyocytes isolated from our gene-targeted mice. However, we also observed increased contractile performance of individual myocytes in isolation, and deletion of PP1β from the heart did positively impact some aspects of cardiac function and performance, such as EDPVR. It should be noted that in our study the effect of loss of *Ppp1cb* on PLN phosphorylation was consistent across 2 different Cre alleles, one of which was adult-specific, with and without isoproterenol stimulation. However, it is possible that loss of PP1β in our study was masked by compensation from the other 2 isoforms, as we did observe increases in PP1α or PP1γ protein levels in the *Ppp1cb* deleted hearts (Fig. 1C and Fig. 6B), which was not reported by Matsuzaki and colleagues [10]. Indeed, even 2 weeks after tamoxifen administration, loss of *Ppp1cb* produced compensatory increases PP1α or PP1γ protein levels, indicating tight regulation of PP1 activity in the heart when a gene targeting approach is used. Further investigation of the role of PP1 on PLN phosphorylation is needed, possibly through combinatorial deleted mice for 2 or 3 of the isoforms at the same time.

One of the major findings in our study is the observed increased phosphorylation of myofilament proteins MLC2V and cMyBPC upon loss of PP1β. MLC2V is a major ventricular sarcomeric protein of approximately 19 kDa associated with the thick filaments, and phosphorylation of MLC2V has been shown to increase cross-bridge cycling kinetics and muscle contraction [47]. Phosphorylation of cMyBPC can also increase cross-bridge cycling kinetics or force production, although the detailed mechanism by which phosphorylation of cMyBPC regulates contraction is not fully understood [48, 49]. Moreover, phosphorylation of cMyBPC is critical for mediating diastolic function through myofilament protein dynamics [50]. In our study, loss of PP1β leads to increased ventricular FS and cell shortening (Figs. 2A,F,G and Figs. 6C,F), consistent with the known function of MLC2V and cMyBPC. However, the disease phenotype in PP1β deficient mice is

contradictory to what is generally known about myofilament protein phosphorylation. Hence, it is possible that phosphorylation status of other unrecognized proteins might contribute to the disease development in PP1β deficient mice or that other phosphorylation sites exist in MLC2V or cMyBPC that have unrecognized functions that are not strictly lusitropic [49]. For example, PP1β may dephosphorylate other potential cMyBPC phosphorylation sites by kinases other than PKA, which could be pathologic [51]. Another possibility is that even a long-term enhancement in lusitropy, such as associated with greater phosphorylation of MLC2V, might ultimately lead to a chronic disease phenotype through unrecognized negative long-term consequences of this enhanced profile.

With respect to isoform compensation, the upregulation of PP1α or PP1γ in the absence of the *Ppp1cb* did not compensate for the effects observed at the level of the myofilament proteins. It is possible that PP1α and PP1γ might be targeted to different locations in the myofilament compared with PP1β, or that these former 2 isoforms are more targeted to the SR microenvironment when compared with PP1β [52].

Hemodynamic assessment using an invasive approach measures blood flow dynamics, while transthoracic echocardiography is a non-invasive method to measure chamber size, thicknesses and ventricular wall movement [53], and clearly each technique has strengths and weaknesses [54, 55]. Mice with PP1β deficiency demonstrated increased contraction in isolated adult myocytes, which was consistent with greater cardiac FS as measured by echocardiography. When the *Ppp1cb* gene was deleted from the adult heart, function as assessed by hemodynamic catheterization showed no effect at baseline, although relaxation rate was significantly augmented (Fig. 7F). This same enhancement in relaxation was observed in individual myocytes (Fig. 2G). However, these adult *Ppp1cb* gene-deleted mice did eventually show cardiac fibrosis and they were unable to increase contractility with dobutamine challenge, suggestive of an associated disease phenotype. Indeed, deletion of the *Ppp1cb* gene with the *Nkx2.5-Cre* allele, which produced an earlier and more extensive loss of PP1β protein, resulted in a baseline reduction in cardiac contractility as assessed with a pressure-volume catheter, with lung congestion and extensive cardiac fibrosis. Hence, loss of PP1β appears to acutely benefit cardiac contractile performance and relaxation, although this appears to have a negative effect long-term on the heart, with significant structural changes such as increased septal wall thickness, enlarged atria and fibrosis. It is likely that aging adult *Ppp1cb* gene deleted mice a number of additional months would show even worse pathology and possibly a contractile deficit at baseline, like the *Ppp1cb* mice with the *Nkx2.5-Cre* allele from an earlier time point.

While the field has diligently attempted to alter PP1 activity in the heart as a surrogate for affecting kinase-mediated phosphorylation of nodal regulatory proteins involved in the “fight-or-flight” response, with the goal of imparting similar beneficial kinetic effects, it seems unlikely that such a strategy will be fruitful based on our observations. Thus, even though PP1β appears to uniquely regulate myofilament phosphorylation levels, it clearly is a required physiologic mediator of proper long-term contractile activity in the heart, such that its continued inhibition would likely lead to disease over time. However, short-term inhibition of PP1β might offer a temporary inotropic benefit to the failing heart by selectively affecting myofilament protein dynamics.

Supplementary Material

Refer to Web version on PubMed Central for supplementary material.

Acknowledgments

Funding Sources

This work was supported by grants from the National Institutes of Health (to J.D. Molkentin). J.D. Molkentin was also supported by the Howard Hughes Medical Institute. R.L., is supported by a training grant from the National Heart Lung and Blood Institute of the NIH (T32HL125204). A.C.N was supported by NIH grant DA10044.

Abbreviations

αMHC	α-myosin heavy chain
cMyBPC	cardiac myosin binding protein C
FS	fractional shortening
I-1	inhibitor 1
I-2	inhibitor 2
IP	intraperitoneal
fl	loxP site
LV	left ventricle
MLC2V	myosin light chain 2V
MLCK	myosin light chain kinase
PKA	protein kinase A
PP1	protein phosphatase 1
PLN	phospholamban
SERCA	sarcoplasmic/endoplasmic reticulum Ca^{2+} ATPase
shRNA	short hairpin RNA
SR	sarcoplasmic reticulum

References

1. Ceulemans H, Bollen M. Functional diversity of protein phosphatase-1, a cellular economizer and reset button. Physiol Rev. 2004; 84:1–39. [PubMed: 14715909]
2. Le AV, Tavalin SJ, Dodge-Kafka KL. Identification of AKAP79 as a protein phosphatase 1 catalytic binding protein. Biochemistry. 2011; 50:5279–5291. [PubMed: 21561082]
3. Bollen M, Peti W, Ragusa MJ, Beullens M. The extended PP1 toolkit: designed to create specificity. Trends in biochemical sciences. 2010; 35:450–458. [PubMed: 20399103]
4. Alessi D, MacDougall LK, Sola MM, Ikebe M, Cohen P. The control of protein phosphatase-1 by targetting subunits. The major myosin phosphatase in avian smooth muscle is a novel form of protein phosphatase-1. European journal of biochemistry / FEBS. 1992; 210:1023–1035. [PubMed: 1336455]

5. Terry-Lorenzo RT, Elliot E, Weiser DC, Prickett TD, Brautigan DL, Shenolikar S. Neurabins recruit protein phosphatase-1 and inhibitor-2 to the actin cytoskeleton. The Journal of biological chemistry. 2002; 277:46535–46543. [PubMed: 12270929]

6. Oliver CJ, Terry-Lorenzo RT, Elliott E, Bloomer WA, Li S, Brautigan DL, et al. Targeting protein phosphatase 1 (PP1) to the actin cytoskeleton: the neurabin I/PP1 complex regulates cell morphology. Molecular and cellular biology. 2002; 22:4690–4701. [PubMed: 12052877]

7. Ragusa MJ, Dancheck B, Critton DA, Nairn AC, Page R, Peti W. Spinophilin directs protein phosphatase 1 specificity by blocking substrate binding sites. Nature structural & molecular biology. 2010; 17:459–464.

8. Mizutani H, Okamoto R, Moriki N, Konishi K, Taniguchi M, Fujita S, et al. Overexpression of myosin phosphatase reduces Ca(2+) sensitivity of contraction and impairs cardiac function. Circulation journal : official journal of the Japanese Circulation Society. 2010; 74:120–128. [PubMed: 19966500]

9. Yamada M, Ikeda Y, Yano M, Yoshimura K, Nishino S, Aoyama H, et al. Inhibition of protein phosphatase 1 by inhibitor-2 gene delivery ameliorates heart failure progression in genetic cardiomyopathy. FASEB J. 2006; 20:1197–1199. [PubMed: 16627625]

10. Aoyama H, Ikeda Y, Miyazaki Y, Yoshimura K, Nishino S, Yamamoto T, et al. Isoform-specific roles of protein phosphatase 1 catalytic subunits in sarcoplasmic reticulum-mediated Ca(2+) cycling. Cardiovasc Res. 2011; 89:79–88. [PubMed: 20675715]

11. Carr AN, Schmidt AG, Suzuki Y, del Monte F, Sato Y, Lanner C, et al. Type 1 phosphatase, a negative regulator of cardiac function. Molecular and cellular biology. 2002; 22:4124–4135. [PubMed: 12024026]

12. Eschenhagen T. Is ryanodine receptor phosphorylation key to the fight or flight response and heart failure? The Journal of clinical investigation. 2010; 120:4197–4203. [PubMed: 21099119]

13. Layland J, Solaro RJ, Shah AM. Regulation of cardiac contractile function by troponin I phosphorylation. Cardiovascular research. 2005; 66:12–21. [PubMed: 15769444]

14. Seguchi O, Takashima S, Yamazaki S, Asakura M, Asano Y, Shintani Y, et al. A cardiac myosin light chain kinase regulates sarcomere assembly in the vertebrate heart. The Journal of clinical investigation. 2007; 117:2812–2824. [PubMed: 17885681]

15. Scruggs SB, Reisdorph R, Armstrong ML, Warren CM, Reisdorph N, Solaro RJ, et al. A novel, in-solution separation of endogenous cardiac sarcomeric proteins and identification of distinct charged variants of regulatory light chain. Molecular & cellular proteomics : MCP. 2010; 9:1804–1818. [PubMed: 20445002]

16. Sanbe A, Fewell JG, Gulick J, Osinska H, Lorenz J, Hall DG, et al. Abnormal cardiac structure and function in mice expressing nonphosphorylatable cardiac regulatory myosin light chain 2. The Journal of biological chemistry. 1999; 274:21085–21094. [PubMed: 10409661]

17. Scruggs SB, Hinken AC, Thawornkaiwong A, Robbins J, Walker LA, de Tombe PP, et al. Ablation of ventricular myosin regulatory light chain phosphorylation in mice causes cardiac dysfunction in situ and affects neighboring myofilament protein phosphorylation. The Journal of biological chemistry. 2009; 284:5097–5106. [PubMed: 19106098]

18. Karsai A, Kellermayer MS, Harris SP. Cross-species mechanical fingerprinting of cardiac myosin binding protein-C. Biophysical journal. 2013; 104:2465–2475. [PubMed: 23746519]

19. Sadayappan S, Osinska H, Klevitsky R, Lorenz JN, Sargent M, Molkentin JD, et al. Cardiac myosin binding protein C phosphorylation is cardioprotective. Proceedings of the National Academy of Sciences of the United States of America. 2006; 103:16918–16923. [PubMed: 17075052]

20. Rosas PC, Liu Y, Abdalla MI, Thomas CM, Kidwell DT, Dusio GF, et al. Phosphorylation of Cardiac Myosin Binding Protein-C is a Critical Mediator of Diastolic Function. Circulation Heart failure. 2015

21. Solaro RJ, Henze M, Kobayashi T. Integration of troponin I phosphorylation with cardiac regulatory networks. Circulation research. 2013; 112:355–366. [PubMed: 23329791]

22. Metzger JM, Westfall MV. Covalent and noncovalent modification of thin filament action: the essential role of troponin in cardiac muscle regulation. Circulation research. 2004; 94:146–158. [PubMed: 14764650]

23. Kirchhefer U, Baba HA, Boknik P, Breeden KM, Mavila N, Bruchert N, et al. Enhanced cardiac function in mice overexpressing protein phosphatase Inhibitor-2. Cardiovascular research. 2005; 68:98–108. [PubMed: 15975567]
24. Pathak A, del Monte F, Zhao W, Schultz JE, Lorenz JN, Bodi I, et al. Enhancement of cardiac function and suppression of heart failure progression by inhibition of protein phosphatase 1. Circulation research. 2005; 96:756–766. [PubMed: 15746443]
25. Grote-Wessels S, Baba HA, Boknik P, El-Armouche A, Fabritz L, Gillmann HJ, et al. Inhibition of protein phosphatase 1 by inhibitor-2 exacerbates progression of cardiac failure in a model with pressure overload. Cardiovascular research. 2008; 79:464–471. [PubMed: 18453636]
26. El-Armouche A, Wittkopper K, Degenhardt F, Weinberger F, Didie M, Melnychenko I, et al. Phosphatase inhibitor-1-deficient mice are protected from catecholamine-induced arrhythmias and myocardial hypertrophy. Cardiovasc Res. 2008; 80:396–406. [PubMed: 18689792]
27. Heijman J, Dewenter M, El-Armouche A, Dobrev D. Function and regulation of serine/threonine phosphatases in the healthy and diseased heart. Journal of molecular and cellular cardiology. 2013; 64:90–98. [PubMed: 24051368]
28. Sinha N, Puri P, Nairn AC, Vijayaraghavan S. Selective ablation of Ppp1cc gene in testicular germ cells causes oligo-teratozoospermia and infertility in mice. Biology of reproduction. 2013; 89:128. [PubMed: 24089200]
29. Moses KA, DeMayo F, Braun RM, Reecy JL, Schwartz RJ. Embryonic expression of an Nkx2-5/Cre gene using ROSA26 reporter mice. Genesis. 2001; 31:176–180. [PubMed: 11783008]
30. Sohal DS, Nghiem M, Crackower MA, Witt SA, Kimball TR, Tymitz KM, et al. Temporally regulated and tissue-specific gene manipulations in the adult and embryonic heart using a tamoxifen-inducible Cre protein. Circulation research. 2001; 89:20–25. [PubMed: 11440973]
31. Kehat I, Davis J, Tiburcy M, Accornero F, Saba-El-Leil MK, Maillet M, et al. Extracellular signal-regulated kinases 1 and 2 regulate the balance between eccentric and concentric cardiac growth. Circulation research. 2011; 108:176–183. [PubMed: 21127295]
32. Yin X, Cuello F, Mayr U, Hao Z, Hornshaw M, Ehler E, et al. Proteomics analysis of the cardiac myofilament subproteome reveals dynamic alterations in phosphatase subunit distribution. Molecular & cellular proteomics : MCP. 2010; 9:497–509. [PubMed: 20037178]
33. Wu X, Chang B, Blair NS, Sargent M, York AJ, Robbins J, et al. Plasma membrane Ca2+-ATPase isoform 4 antagonizes cardiac hypertrophy in association with calcineurin inhibition in rodents. The Journal of clinical investigation. 2009; 119:976–985. [PubMed: 19287093]
34. Coutu P, Metzger JM. Genetic manipulation of calcium-handling proteins in cardiac myocytes. II. Mathematical modeling studies. American journal of physiology Heart and circulatory physiology. 2005; 288:H613–H631. [PubMed: 15331371]
35. Davis J, Wen H, Edwards T, Metzger JM. Thin filament disinhibition by restrictive cardiomyopathy mutant R193H troponin I induces Ca2+-independent mechanical tone and acute myocyte remodeling. Circulation research. 2007; 100:1494–1502. [PubMed: 17463320]
36. Porterfield JE, Kottam AT, Raghavan K, Escobedo D, Jenkins JT, Larson ER, et al. Dynamic correction for parallel conductance, GP, and gain factor, alpha, in invasive murine left ventricular volume measurements. J Appl Physiol (1985). 2009; 107:1693–1703. [PubMed: 19696357]
37. Liu Q, Chen X, Macdonnell SM, Kranias EG, Lorenz JN, Leitges M, et al. Protein kinase C{alpha}, but not PKC{beta} or PKC{gamma}, regulates contractility and heart failure susceptibility: implications for ruboxistaurin as a novel therapeutic approach. Circulation research. 2009; 105:194–200. [PubMed: 19556521]
38. Oka T, Maillet M, Watt AJ, Schwartz RJ, Aronow BJ, Duncan SA, et al. Cardiac-specific deletion of Gata4 reveals its requirement for hypertrophy, compensation, and myocyte viability. Circulation research. 2006; 98:837–845. [PubMed: 16514068]
39. Maillet M, Davis J, Auger-Messier M, York A, Osinska H, Piquereau J, et al. Heart-specific deletion of CnB1 reveals multiple mechanisms whereby calcineurin regulates cardiac growth and function. The Journal of biological chemistry. 2010; 285:6716–6724. [PubMed: 20037164]
40. Scruggs SB, Solaro RJ. The significance of regulatory light chain phosphorylation in cardiac physiology. Arch Biochem Biophys. 2011; 510:129–134. [PubMed: 21345328]

41. Satoh M, Ogita H, Takeshita K, Mukai Y, Kwiatkowski DJ, Liao JK. Requirement of Rac1 in the development of cardiac hypertrophy. Proceedings of the National Academy of Sciences of the United States of America. 2006; 103:7432–7437. [PubMed: 16651530]

42. Raake PW, Vinge LE, Gao E, Boucher M, Rengo G, Chen X, et al. G protein-coupled receptor kinase 2 ablation in cardiac myocytes before or after myocardial infarction prevents heart failure. Circulation research. 2008; 103:413–422. [PubMed: 18635825]

43. Burkhoff D, Mirsky I, Suga H. Assessment of systolic and diastolic ventricular properties via pressure-volume analysis: a guide for clinical, translational, and basic researchers. Am J Physiol Heart Circ Physiol. 2005; 289:H501–H512. [PubMed: 16014610]

44. Nicolaou P, Hajjar RJ, Kranias EG. Role of protein phosphatase-1 inhibitor-1 in cardiac physiology and pathophysiology. Journal of molecular and cellular cardiology. 2009; 47:365–371. [PubMed: 19481088]

45. Chiang DY, Lebesgue N, Beavers DL, Alsina KM, Damen JM, Voigt N, et al. Alterations in the interactome of serine/threonine protein phosphatase type-1 in atrial fibrillation patients. J Am Coll Cardiol. 2015; 65:163–173. [PubMed: 25593058]

46. Miyazaki Y, Ikeda Y, Shiraishi K, Fujimoto SN, Aoyama H, Yoshimura K, et al. Heart failure-inducible gene therapy targeting protein phosphatase 1 prevents progressive left ventricular remodeling. PloS one. 2012; 7:e35875. [PubMed: 22558250]

47. Sheikh F, Ouyang K, Campbell SG, Lyon RC, Chuang J, Fitzsimons D, et al. Mouse and computational models link Mlc2v dephosphorylation to altered myosin kinetics in early cardiac disease. J Clin Invest. 2012; 122:1209–1221. [PubMed: 22426213]

48. Sheikh F, Lyon RC, Chen J. Getting the skinny on thick filament regulation in cardiac muscle biology and disease. Trends in cardiovascular medicine. 2014; 24:133–141. [PubMed: 23968570]

49. Moss RL, Fitzsimons DP, Ralphe JC. Cardiac MyBP-C regulates the rate and force of contraction in mammalian myocardium. Circ Res. 2015; 116:183–192. [PubMed: 25552695]

50. Tong CW, Nair NA, Doersch KM, Liu Y, Rosas PC. Cardiac myosin-binding protein-C is a critical mediator of diastolic function. Pflugers Archiv : European journal of physiology. 2014; 466:451–457. [PubMed: 24442121]

51. Kotlo K, Johnson KR, Grillon JM, Geenen DL, deTombe P, Danziger RS. Phosphoprotein abundance changes in hypertensive cardiac remodeling. J Proteomics. 2012; 77:1–13. [PubMed: 22659219]

52. Yang F, Aiello DL, Pyle WG. Cardiac myofilament regulation by protein phosphatase type 1alpha and CapZ. Biochem Cell Biol. 2008; 86:70–78. [PubMed: 18364747]

53. Huang SJ, McLean AS. Appreciating the strengths and weaknesses of transthoracic echocardiography in hemodynamic assessments. Cardiol Res Pract. 2012; 2012:894308. [PubMed: 22454777]

54. Kirkpatrick JN, Vannan MA, Narula J, Lang RM. Echocardiography in heart failure: applications, utility, and new horizons. J Am Coll Cardiol. 2007; 50:381–396. [PubMed: 17662389]

55. Nishimura RA, Carabello BA. Hemodynamics in the cardiac catheterization laboratory of the 21st century. Circulation. 2012; 125:2138–2150. [PubMed: 22547754]

Highlights

- Deletion of PP1β protein from the heart results in concentric remodeling
- Deletion of PP1β protein from the heart leads to contractile dysfunction
- PP1β is targeted to the myofilaments over other PP1 isoforms
- Loss of PP1β increases phosphorylation of select myofilament proteins
- Individual deletion of PP1α, PP1β or PP1γ does not alter PLN phosphorylation
- Loss of PP1β from the heart does not affect myocyte Ca^{2+} handling

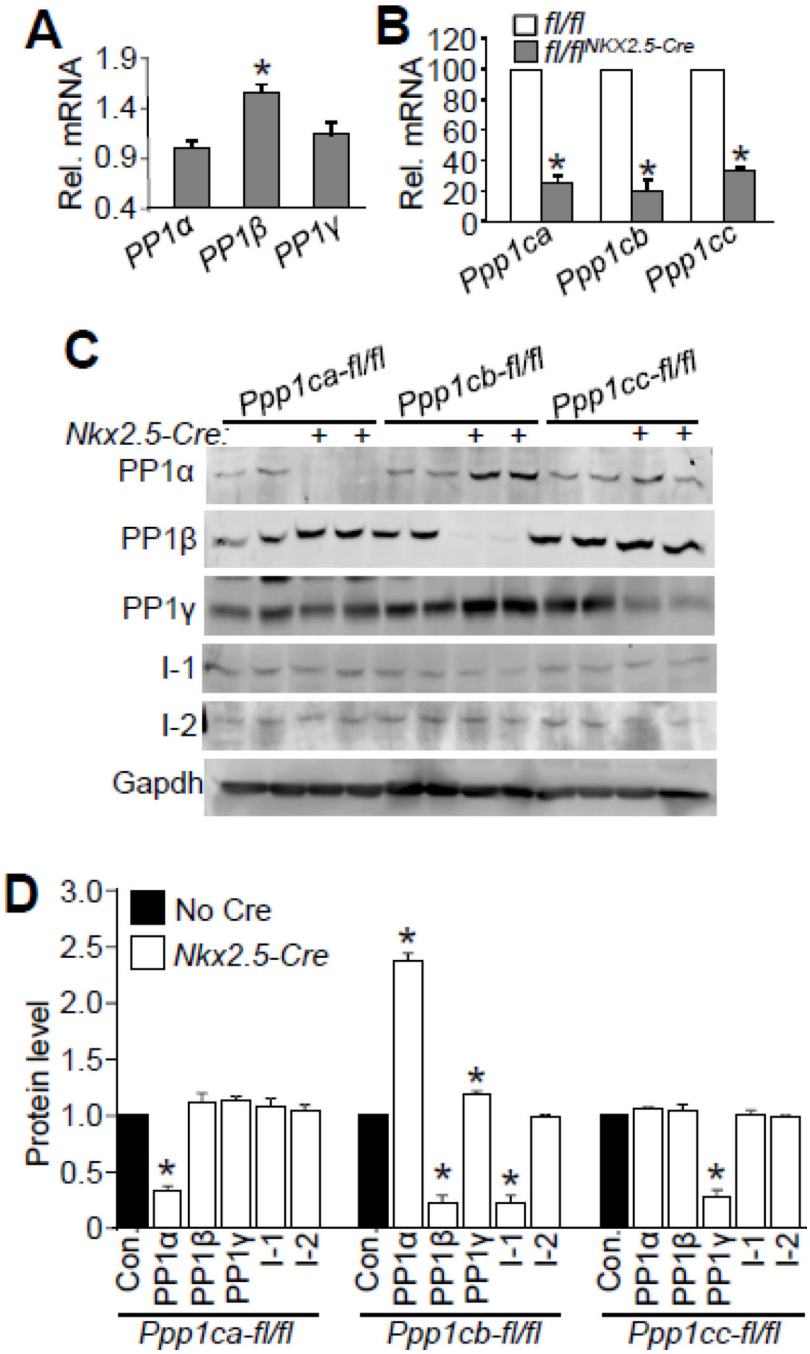

Figure 1. Generation and assessment of cardiac specific PP1 isoform deleted mice

(A) Real-time PCR analysis of expression of PP1 isoforms in adult cardiac myocytes. Rpl27 was used as an internal control. N=3 for each group. *p<0.05 vs PP1α. (B) Realtime PCR analysis of expression of PP1 isoforms in the hearts of 2 month-old mice for each of the groups shown, with or without Cre-mediated deletion. N=4 for each group in the real-time PCR analysis. *p<0.05 *vs fl/fl* mice. (C) Western blots for PP1 isoforms, I-1, I-2, and gapdh from the hearts of *Ppp1c-fl/fl* mice or *Ppp1c-fl/fl*$^{Nkx2.5\text{-}Cre}$ mice. Approximately 120 μg of

protein was processed to detect I-1 and I-2. D) Quantification of Western blots shown in Figure 1C. N=4 for each of the groups. *p<0.05 vs control (Con.).

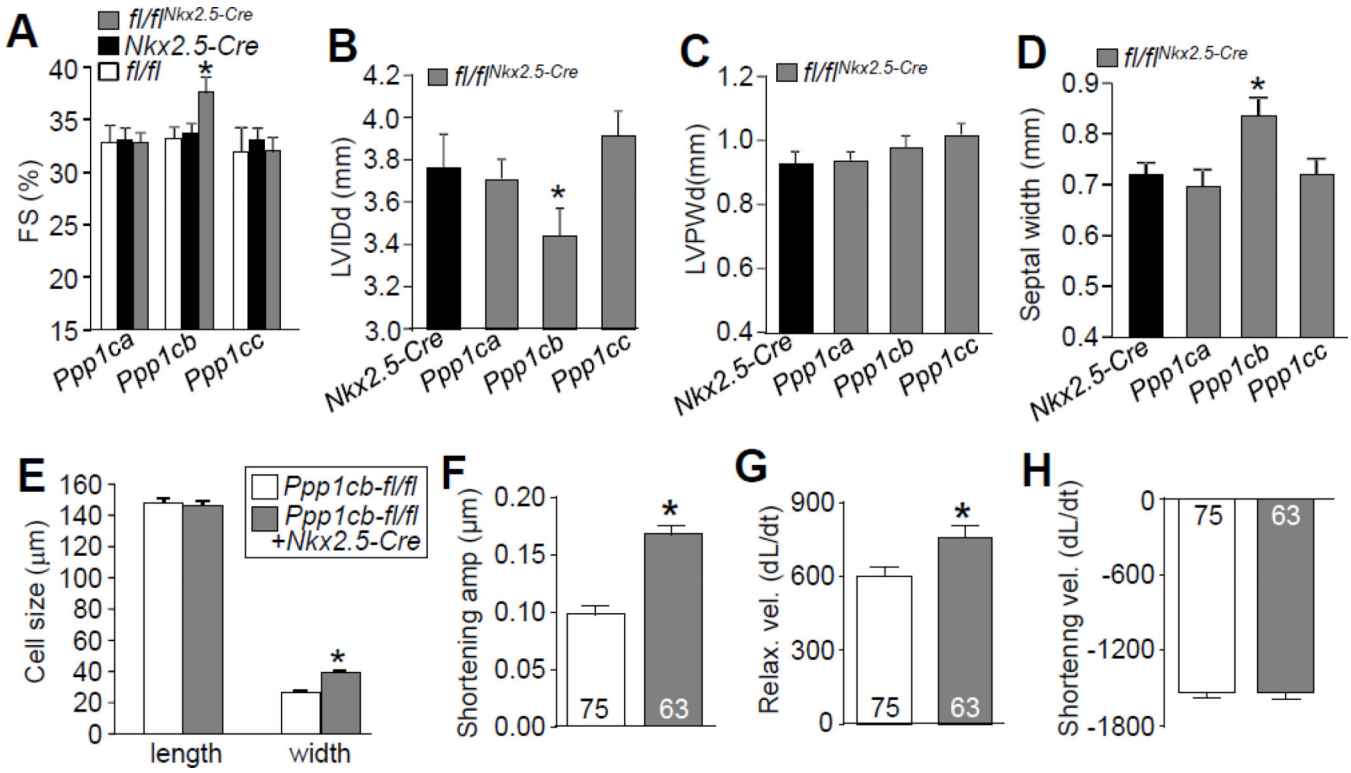

Figure 2. Cardiac deletion of PP1β leads to enhanced contraction and cardiac remodeling

(A–D) Echocardiographic measurements of 2 month-old mice for fractional shortening (FS %), left ventricular internal diastolic dimension (LVIDd), left ventricular posterior wall dimension(LVPWd), and septal width. N=10 for each group. *p<0.05 vs *Nkx2.5-Cre*. (E) Length and width of 224 adult cardiac myocytes isolated from 2 month-old mice of the indicated genotypes, measured by NIH ImageJ software.*p< 0.05 vs *Ppp1cb-fl/fl.(F–H)* Shortening amplitude, relaxation velocity, and shortening velocity in isolated adult cardiomyocyte from the hearts of the indicated genotypes of mice. *p<0.05 vs *Ppp1cb-fl/fl*. Data are normalized to the peak of their shortening amplitude, and units are µm/second for change in length (dL) per change in time (dt).

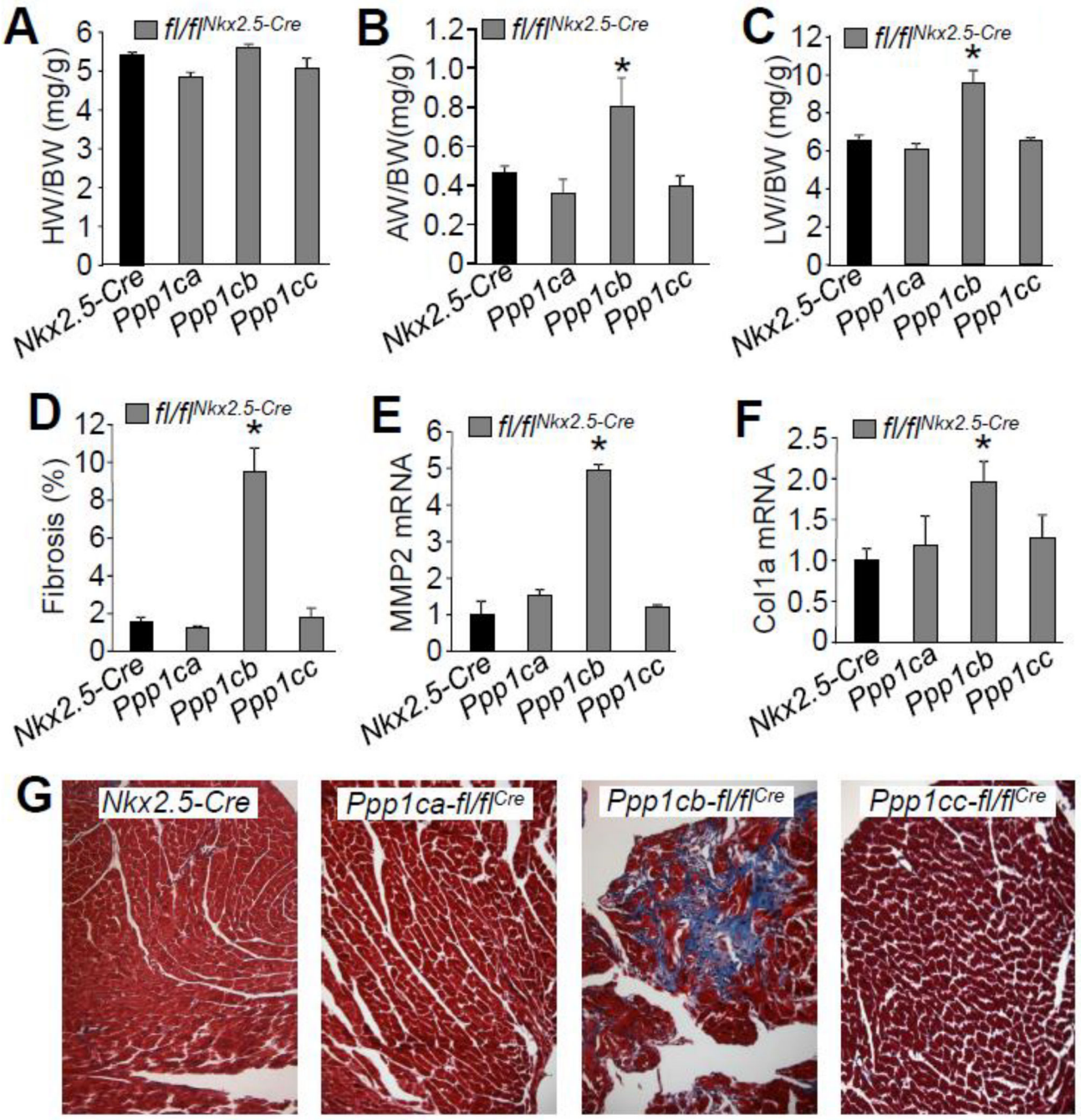

Figure 3. Cardiac deletion of PP1β results in interstitial fibrosis and heart failure

(A–C) Measurements of heart weight/body weight (HW/BW), atria weight/body weight (AW/BW), and lung weight/body weight (LW/BW) in the indicated groups of mice, assayed at 2 months of age. N=8 for each group of mice. (D) Percentage of interstitial fibrosis from the hearts of the indicated mice, as quantified using MetaMorph software based on Masson's trichrome-stained heart histological sections as shown in panel G. Images from at least 4 hearts in each group were used for analysis. (E–F) Quantitative PCR analysis of expression of MMP2 and collagen 1 α1 using total RNAs purifed from hearts of each of the groups

indicated (N=3). (F) Representative histological sections stained with Masson's trichrome (shows fibrosis in blue) from the hearts of the indicated genotypes of mice. *p<0.05 *vs* *Nkx2.5-Cre* for all panels.

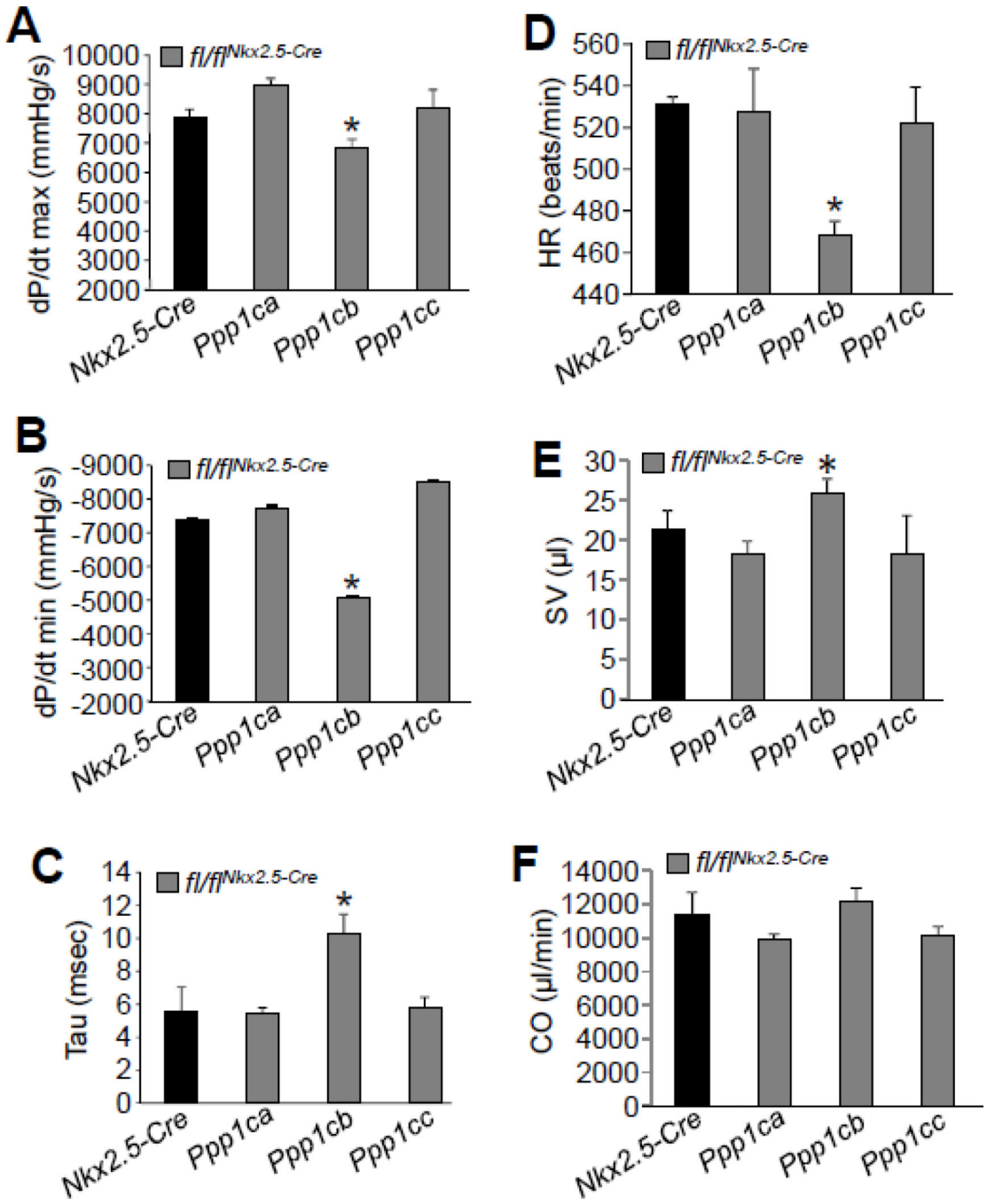

Figure 4. Cardiac deletion of PP1β protein results in contractile dysfunction

(A–B) Invasive hemodynamic measurement of cardiac contractility assessed at baseline (load-dependent) as maximum and minimum rate of pressure change in the left ventricle over time (dP/dt max and dP/dt min, respectively) in *Nkx2.5-Cre* control mice versus *Ppp1ca-fl/fl*$^{Nkx2.5\text{-}Cre}$, *Ppp1cb-fl/fl*$^{Nkx2.5\text{-}Cre}$, and *Ppp1cc- fl/fl*$^{Nkx2.5\text{-}Cre}$ containing mice (C) Time constant for isovolumetric relaxation (Tau) showing the exponential decay of ventricular pressure during isovolumic relaxation. (D–F) Analysis of heart rate (HR), stroke volume (SV), and cardiac output (CO) from the hemodynamic measurements in the

indicated genotypes of mice. At least 3 mice for each group were used for the measurements. *p<0.05 *vs Nkx2.5-Cre*.

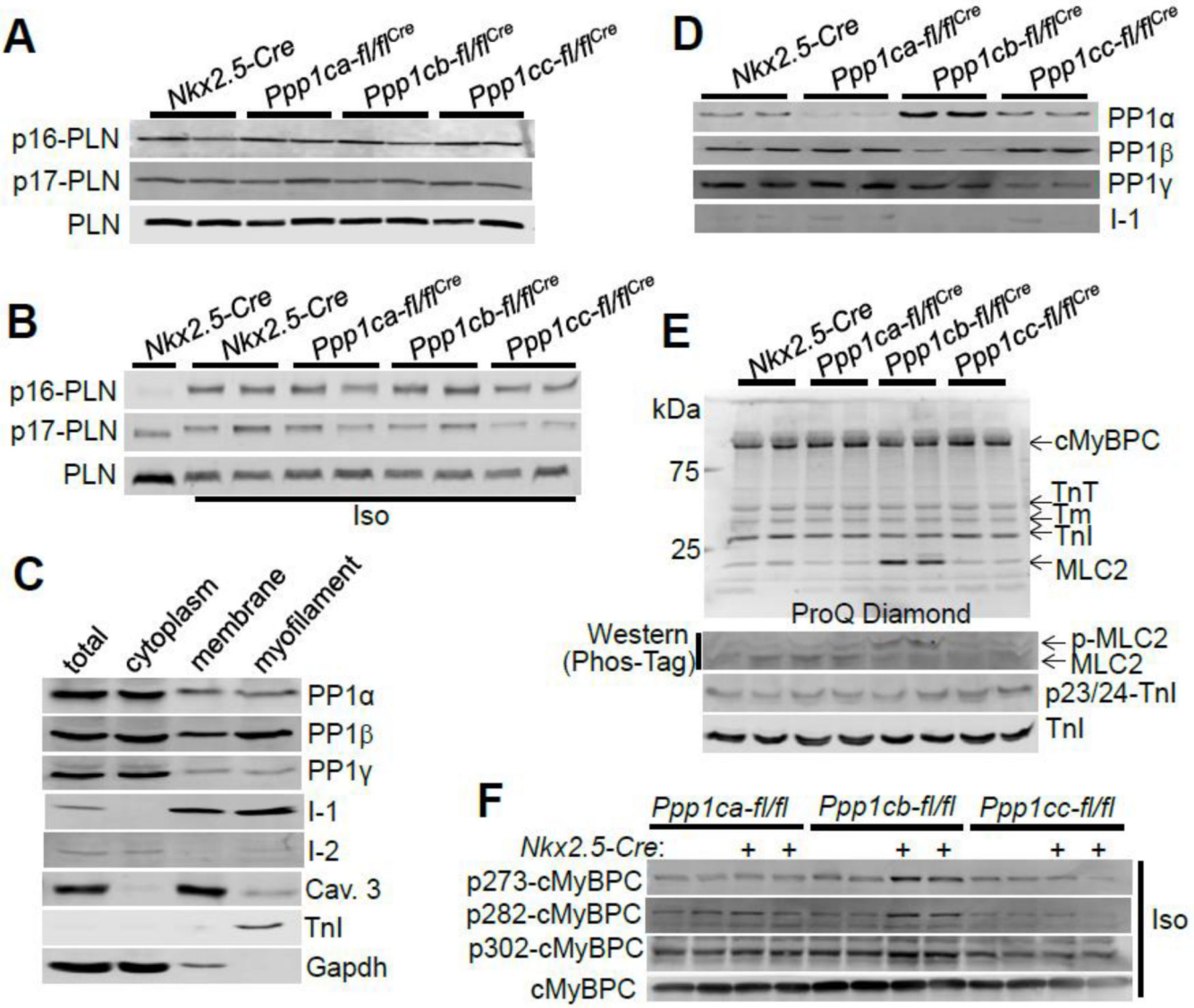

Figure 5. Myofilament localization of PP1β influences phosphorylation of MLC2V and cMyBPC without affecting PLN

(A–B) Western blot for phospho-PLN and total PLN from the hearts of the indicated groups at baseline or upon isoproterenol (Iso) challenge for 10 minutes. (C) Western blot for the localization of each of the indicated proteins in the indicated protein subfractions from adult cardiac myocytes. (D) Western blot for the indicated proteins in myofilament protein fractions using hearts from each of the indicated genotypes. (E) Upper gel, ProQ-Diamond staining of myofilament proteins for their phosphorylation status. Lower gel, detection of phosphorylation of MLC2V by Phos-Tag gel and Western blotting using an MLC2V antibody. Phosphorylation of troponin I was detected with pSer23/24 specific antibody. The upward shifted phosphorylated MLC2V protein is observed with loss of PP1β. Abbreviations: TnT, troponin T; Tm, tropomyosin; TnI, troponin I. (F) Western blotting of cMyBPC phosphorylation from the hearts of the indicated groups of mice administered isoproterenol (Iso, 20 μg/g) for 10 min.

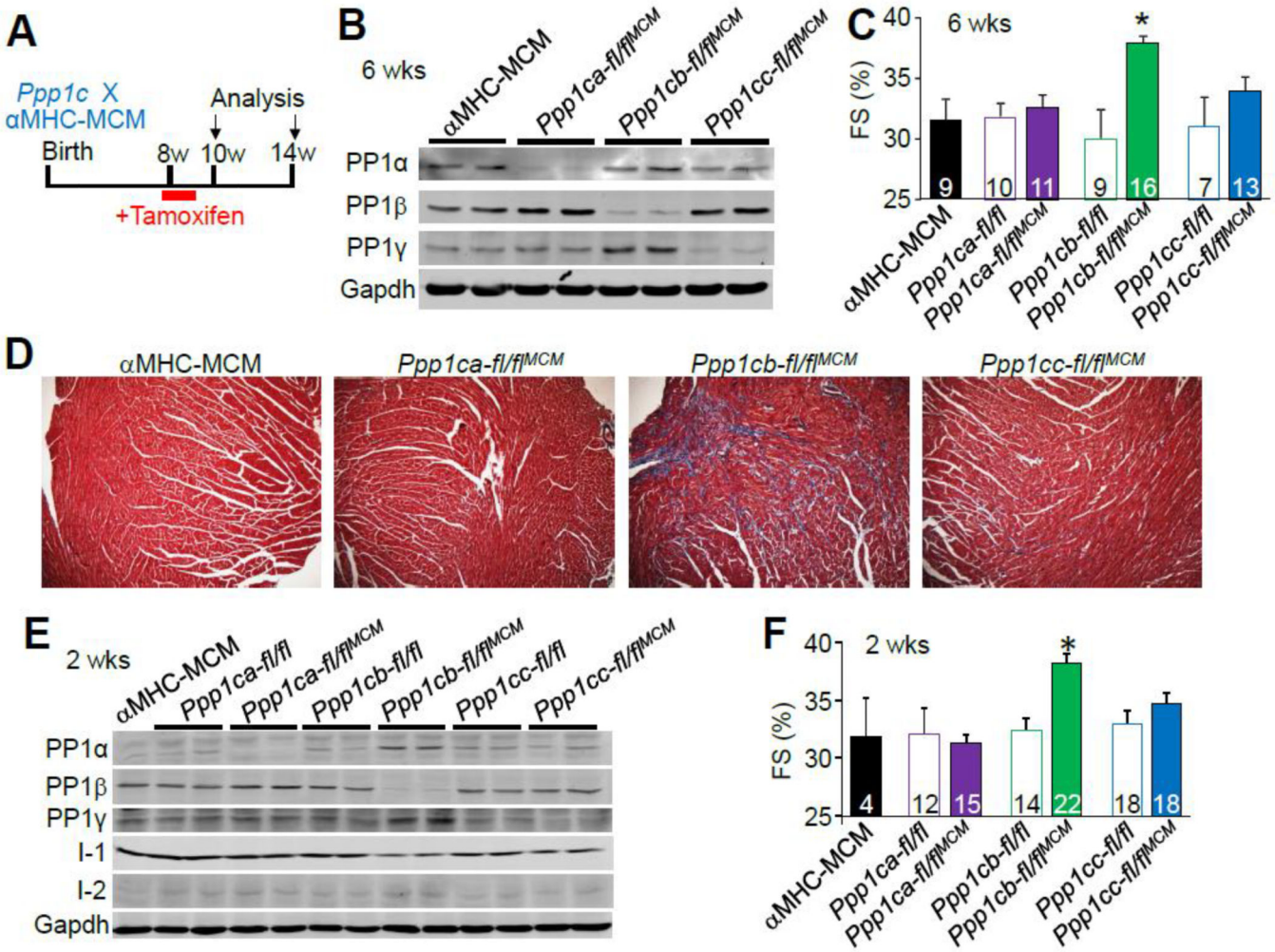

Figure 6. Adult deletion of PP1 isoforms byc *αMHC-MerCreMer* and the effects on cardiac function and interstitial fibrosis

(A) Schematic representation of the experimental setup. Eight week-old mice were administered five consecutive days of tamoxifen (0.5 mg/day) and then analyzed at 10 and 14 weeks of age. (B) Western blot for PP1 isoform deletion from cardiac protein extracts in each of the indicated genotypes of mice 6 weeks after the start of tamoxifen treatment. (C) Echocardiographic measurement of cardiac fractional shortening (FS%) of the indicated genotypes of mice 6 weeks after tamoxifen administration. *p<0.05 *vs αMHC-MerCreMer*. Number of mice used is shown in the bars. (D) Masson's trichrome staining of paraffin-embedded heart sections from *αMHC-MerCreMer* controls and the indicated *Ppp1c*-deleted mice. (E) Western blot for PP1 isoform deletion from cardiac protein extracts in each of the indicated genotypes of mice 2 weeks after the start of tamoxifen treatment. (F) Echocardiographic measurement of cardiac fractional shortening (FS%) of the indicated genotypes of mice 2 weeks after tamoxifen administration. *p<0.05 *vs αMHC-MerCreMer*. Number of mice used is shown within the bars. Abbreviations, MCM, aMHC-MerCreMer transgene.

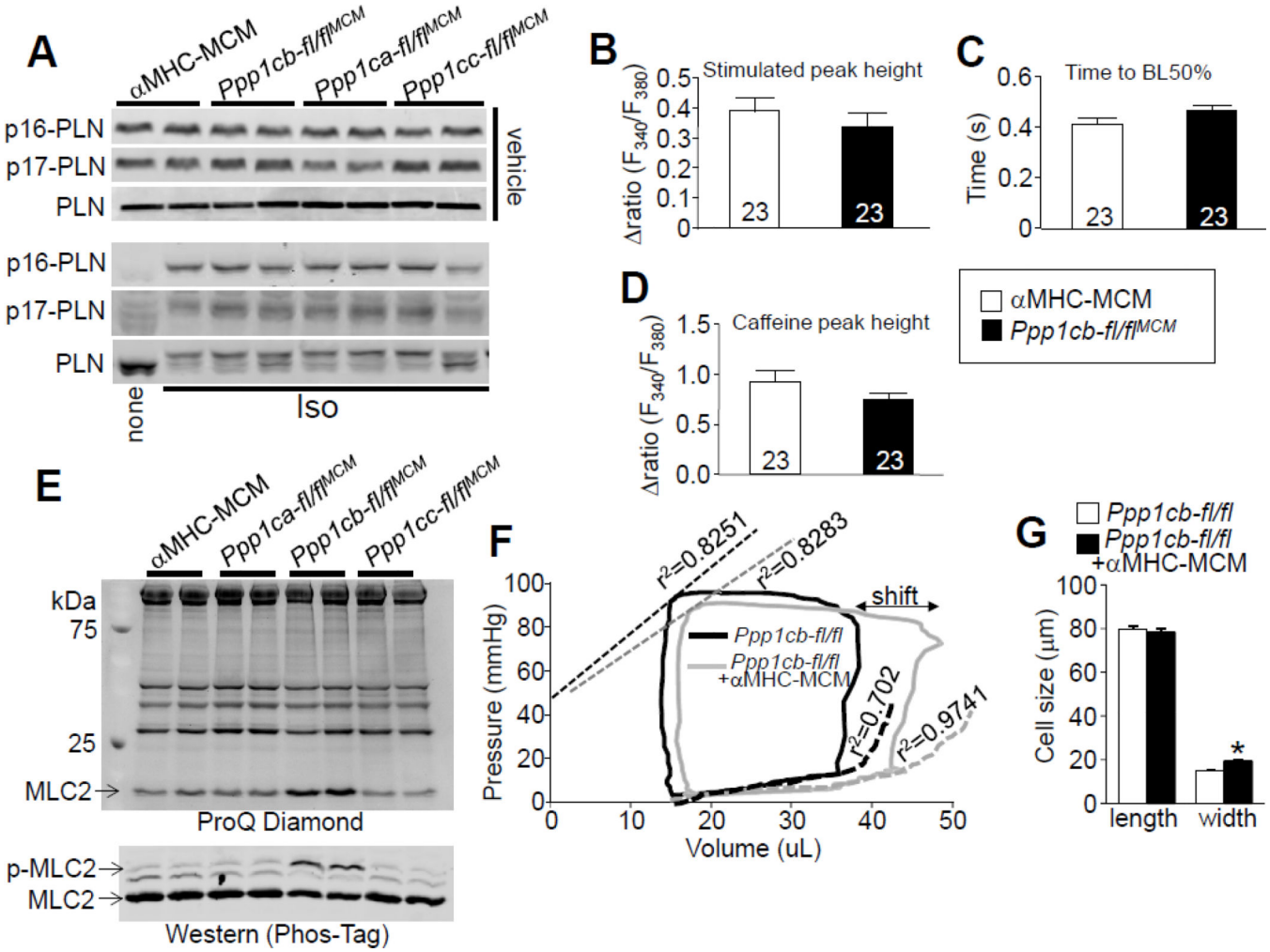

Figure 7. Effect of adult-specific PP1β deletion on protein phosphorylation, Ca^{2+} handling, and cardiac performance

(A) Western blotting for phospho-PLN and total PLN from adult cardiac myocytes isolated from indicated genotypes of mice 6 weeks after tamoxifen treatment with vehicle (upper) or isoproterenol (Iso) treatment (lower). (B) Mean maximal amplitude of electrically-evoked Ca^{2+} transients in adult cardiomyocytes from *aMHC-MerCreMer* control or *Ppp1cb-fl/fl*^{MCM} mice, as well as (C) Ca^{2+} decay time and the (D) mean maximal Ca^{2+} response to acute caffeine treatment. Number of cells analyzed is shown within the bars of each graph. (E) Upper gel, ProQ-Diamond staining of myofilament proteins for their phosphorylation from hearts of the indicated genotypes of mice 6 weeks after tamoxifen treatment. Lower gel, detection of MLC2V phosphorylation by Phos-Tag gel and western blotting with MLC2V antibody from cardiac protein extracts of the same groups of mice. (F) Representative baseline cardiac pressure-volume loops obtained by invasive hemodynamic measurements in *Ppp1cb-fl/fl* and *Ppp1cb-fl/fl*^{MCM} mice 2 weeks post tamoxifen treatment. The “shift” indicated on the figure shows a diastolic alteration. Abbreviations, ESPVR, end systolic pressure-volume relationship; EDPVR, end diastolic pressure-volume relationship (N=6,7 mice of each genotype). (G) Length and width of adult myocytes isolated from the hearts of the indicated mice 6 weeks after tamoxifen treatment. Exactly 113 myocytes from

each group were measured using ImageJ software. *p<0.05 *vs Ppp1cb-fl/fl*. Abbreviations, MCM, αMHC-MerCreMer transgene.